



**HAL**  
open science

# Investigating the thermal effects of plasma surface treatment on crystallinity and mechanical behavior of PEEK

Ahmad Al Khatib, Raphaël Le Franc, Jean-Pierre Guin, Jean-François Coulon

► **To cite this version:**

Ahmad Al Khatib, Raphaël Le Franc, Jean-Pierre Guin, Jean-François Coulon. Investigating the thermal effects of plasma surface treatment on crystallinity and mechanical behavior of PEEK. *Polymer Degradation and Stability*, 2023, 216, pp.110500. 10.1016/j.polymdegradstab.2023.110500. hal-04195312

**HAL Id: hal-04195312**

**<https://hal.science/hal-04195312>**

Submitted on 22 Sep 2023

**HAL** is a multi-disciplinary open access archive for the deposit and dissemination of scientific research documents, whether they are published or not. The documents may come from teaching and research institutions in France or abroad, or from public or private research centers.

L'archive ouverte pluridisciplinaire **HAL**, est destinée au dépôt et à la diffusion de documents scientifiques de niveau recherche, publiés ou non, émanant des établissements d'enseignement et de recherche français ou étrangers, des laboratoires publics ou privés.

## Investigating the thermal effects of plasma surface treatment on crystallinity and mechanical behavior of PEEK

---

Ahmad AL KHATIB<sup>1</sup>, Raphaël LE-FRANC<sup>1</sup>, Jean-Pierre GUIN<sup>2</sup>, Jean-François COULON<sup>1</sup> \*

<sup>1</sup> ECAM RENNES – Louis de Broglie, Campus de Ker Lann, CS 29 128, 35091 Rennes Cedex 09, France

<sup>2</sup> Institut de Physique de Rennes, Univ Rennes, CNRS IPR-UMR 62051, F-35000 Rennes, France

### **ABSTRACT**

This study investigates the influence of plasma surface treatment on the local crystallinity and its impact on the local and global mechanical properties of PEEK samples. Local degree of crystallinity is assessed using Raman spectroscopy, while nanoindentation measurements are employed to examine the nanoscale mechanical properties for commercial, raw injected, annealed, and plasma-treated PEEK samples. The results reveal a significant correlation between the local degree of crystallinity and the nanoscale mechanical properties within the PEEK cross-section. Scanning electron microscopy (SEM) observations further support these findings by illustrating the density and evolution of spherulitic structures within the PEEK cross-section. Tensile mechanical tests are conducted to evaluate the influence of crystallinity variation on overall behavior. The results demonstrate that even localized variations in crystallinity can affect the overall mechanical response of PEEK samples. These findings enhance our understanding of the relationship between crystallinity, mechanical properties, and surface treatment on PEEK, providing valuable insights for optimizing its performance in various applications.

**Keywords:** PEEK, Crystallization, Nanoindentation, Plasma treatment, Mechanical properties

## 1. Introduction

In the global environmental emergency to reduce the impact of fossil fuels, the demand for lightweight materials has significantly increased to replace conventional materials such as metals, in order to mutate to green concepts. Among these materials, thermoplastic-based composites are widely employed for numerous applications due to their recyclability, high mechanical performance, and rapid processability [1,2]. Semicrystalline high-performance thermoplastics, such as poly(ether-ether-ketone) (PEEK), have been extensively researched for many years due to their exceptional properties, including high thermal, mechanical, chemical, wear, and radiation resistance. These properties make them ideal for applications subjected to severe operating conditions [3]. PEEK also possesses an excellent mechanical strength-to-weight ratio. These remarkable properties position PEEK as a viable candidate to replace metallic components in various applications, including automotive, aerospace, and medical fields.

However, adhesion to PEEK, like most polymers, is limited by its relatively low surface free energy. This poses a challenge for the assembly of mechanical parts across various applications. Consequently, numerous physical and/or chemical surface treatments have been investigated to enhance the wettability and adhesion capabilities of PEEK [4–7]. Among these treatments, cold plasma technologies have emerged as a promising approach to improve adhesion strength on PEEK by employing one or both of the following adhesion mechanisms: functionalization and mechanical anchorage [8–13]. Despite this adhesion improvement, concerns may arise regarding potential alterations in the crystallization and mechanical behavior of the polymer caused by the inherent thermal effects of these surface treatments.

The crystallization of PEEK has been the subject of numerous studies over the years. In particular, the crystallization ratio is dependent on the thermal history and the conditions of thermal treatment [14,15]. The thermal history of PEEK influences the thickness of the lamellae, as well as the size and density of the spherulites [15–20]. The degree of crystallinity  $\chi_c$  is commonly determined using various techniques such as Differential Scanning Calorimetry (DSC), X-Ray Diffraction (XRD), density measurement, and Raman spectroscopy. Recent studies have highlighted that Raman spectroscopy seems to be a very relevant technique to determine the local crystallinity on the surface of the sample [21,22].

The thermal history experienced by PEEK during processing influences its macroscopic mechanical properties [23]. Fast quenched amorphous samples exhibited the highest toughness and the greatest strain before rupture. On the other hand, samples cooled slowly (with approximately 33% crystallinity) demonstrated higher stress at yield and neck propagation compared to the amorphous samples, but a lower breaking strain. This behavior was attributed to the difference in crystallinity between these sample types. Furthermore, static flexural tests conducted on PEEK and carbon fiber reinforced (CFR) PEEK composite samples revealed a significant correlation between the flexural peak load and the crystalline content obtained by different annealing temperatures [24]. More recently, this correlation has also been observed in treated samples of 3D printed short carbon fiber reinforced (CFR) PEEK composites [25]. Higher crystallinity results in increased tensile strength, tensile modulus, flexural strength, and flexural modulus. Additionally, process parameters such as the ambient temperature during 3D printing can affect crystallinity and mechanical properties.

Nanoindentation is a nano-length scale mechanical characterization technique for measuring the near-surface mechanical properties. It offers a valuable nondestructive, rapid, and reproducible approach, not only applicable to metallic materials but also to polymers.

Recent studies have explored the local surface mechanical response, including hardness and elastic modulus, of PEEK and PEEK composites using nanoindentation. These investigations focused on different treatments such as quenching and annealing [26–30]. Using this technique, a bimodal character of the semicrystalline PEEK was observed due to the presence of hard crystalline lamella within a softer amorphous phase [26]. It has been observed that the surface mechanical properties of the semicrystalline polymers depend on the degree of crystallinity. A higher global crystalline content in PEEK samples corresponds to enhanced mechanical properties (hardness and elastic modulus) at the surface as measured by nanoindentation [26,28]. This correlation between crystallinity and nanoindentation measurements was also observed on PEEK and CFR PEEK composite for varying annealing temperatures [24,30]. However, this correlation was less pronounced in CFR-PEEK than in PEEK, mainly due to the complex microstructure of carbon fiber reinforced composites. Surface properties of semicrystalline PEEK, such as high surface roughness and the presence of inhomogeneous crystallinity throughout the sample thickness, can influence nanoindentation measurements and lead to notable anomalies [28]. Mechanical polishing can enhance the results with minimal residual stress on PEEK [28]. Furthermore, annealing techniques reduce the surface crystallinity heterogeneity and lead to acceptable results [28].

The main inquiry addressed in this paper pertains to the potential impact of thermal effects resulting from surface treatments, specifically plasma treatment, on the crystallinity and mechanical properties of PEEK. Indeed, little is known regarding the variation in crystallinity throughout the depth of plasma-treated samples and its consequential effects on the mechanical properties of PEEK. This paper focuses on examining the variation in crystallinity through the cross-section of PEEK samples, including as-received commercial samples, injection molded samples, surface plasma-treated samples, and thermally annealed samples. The study investigates the influence of crystallinity variation on both nanoscale and macroscopic

mechanical properties. To achieve this, a combination of global and local approaches is employed. The global approach involves macroscopic mechanical tensile tests and measurement of global crystallinity using density analysis. On the other hand, the local approach relies on nanoindentation to obtain nanoscale mechanical properties of PEEK, Raman spectroscopy to assess local crystallinity, and Scanning Electron Microscopy (SEM) for observing the morphology of PEEK.

## **2. Material and methods**

### **2.1. PEEK samples**

Two types of PEEK samples were employed in these experiments. The first type consisted of as-received commercial PEEK obtained as 3 mm thick sheets from a commercial supplier (VICTREX<sup>®</sup> PEEK<sup>™</sup> 600G). These sheets were cut into 50 × 25 mm<sup>2</sup> rectangles to facilitate handling during the various experiments. This PEEK will be referred to as 'commercial PEEK' hereafter and served as the reference for the study.

The second type was produced in our laboratory using purchased granules (VICTREX<sup>®</sup> PEEK<sup>™</sup> 450G) and fabricated into tensile specimens following the ISO 527/2-5A standard (2 mm thickness). The granules were stored and dried in a desiccator to remove any residual moisture before being injection molded at a nozzle temperature of 410°C, which is above the melting temperature of PEEK ( $T_m = 343^\circ\text{C}$ ). Intentionally, the mold was not preheated to deliberately induce variation in crystallinity across the cross-section of the specimens. This was achieved through rapid cooling between the injection nozzle and the mold temperature. Henceforth, these specimens will be referred to as 'injected PEEK'.

Both PEEK grades, 600G and 450G, are suitable for injection molding and extrusion processes. The PEEK 450G grade is considered as a standard flow general-purpose material,

with a viscosity of 350 Pa.s at 400°C. On the other hand, the PEEK 600G grade is classified as a low flow general-purpose material, with a viscosity of 500 Pa.s at 400°C.

Building upon the studies conducted by Martineau et al. [31] and Doumeng and al. [21], some of the injected PEEK samples were subjected to annealing to induce cold crystallization at two different temperatures: 180°C and 250°C. These temperatures were selected to ensure they were above the glass transition temperature ( $T_g = 143^\circ\text{C}$ ) but below the melting temperature ( $T_m = 343^\circ\text{C}$ ). The specimens were gradually heated in a programmable oven, maintained at the designated annealing temperature for 20 minutes, and then rapidly quenched using liquid nitrogen for 1 minute to stop the crystallization process. Consequently, these specimens will henceforth be referred to as '180°C annealed PEEK' and '250°C annealed PEEK' respectively.

Furthermore, the injected PEEK samples underwent surface treatment using an atmospheric pressure plasma system (Ultra-Light System from AcXys™). The discharge voltage applied was 1.5 kV, operating at a low frequency of 100 kHz. The plasma torch was positioned 2 cm above the specimen and moved at a forward speed of 10 mm/s. The treatment parameters were determined based on the study of Gravis et al. [13] to optimize adhesion enhancement on PEEK surfaces. During the plasma treatment, the surface temperature of the material was monitored using a thermal imaging camera. The highest observed surface temperature reached 280°C, surpassing the glass transition temperature ( $T_g = 143^\circ\text{C}$ ). It is important to indicate that the atmospheric pressure plasma treatment used in this study results in a significant elevation in the surface concentration of C-O (ketone) and COO (ester/acid) functional groups, while the concentration of C-O-C (ether) remains relatively constant [11]. This modification in the surface chemistry, discussed in our previous study, leads to an increase in the surface free energy contributing to enhance the practical adhesion on the PEEK surface. Henceforth, these specimens will be referred to as 'plasma-treated PEEK'

## 2.2. Crystallinity measuring

The global degree of crystallinity was determined through density measurements with an immersion technique according to the ISO 1183–1:2019 standard. A PCE-AB C balance with a precision of 0.1 mg was utilized for the measurements. Each specimen was weighed five times to ensure reproducibility. The global degree of crystallinity ( $\chi_c$ ) is calculated from the equation (1), which incorporates the theoretical densities of the amorphous phase ( $\rho_a = 1.263 \text{ g.cm}^{-3}$ ) and the crystalline phase ( $\rho_c = 1.400 \text{ g.cm}^{-3}$ ) as described by Blundell and Osborn [32].

$$\chi_c = \frac{\rho - \rho_a}{\rho_c - \rho_a} \quad (1)$$

Here,  $\rho$  represents the density of the sample measured using the immersion technique.

The local degree of crystallinity at different points in the cross-section of PEEK specimen was measured using Raman spectrometer WiTec's Apyron 300R. The analysis parameters included a laser wavelength of 785 nm, laser power of 42.328 mW, 10 scans number, and an integration time of 8 seconds. The obtained Raman spectra were then analyzed using the OriginPro<sup>®</sup> software in order to bring out the degree of crystallinity of the PEEK. Specifically, the zone of interest, as identified by Doumeng and al. [21], was around 1600  $\text{cm}^{-1}$ . The  $A_{1607/1595}$  ratio, which represents the ratio of the areas under the peaks located at 1607 and 1595  $\text{cm}^{-1}$ , showed a strong correlation with the degree of crystallinity of PEEK. By deconvoluting these two peaks using OriginPro<sup>®</sup> and applying the correlation curve [21], we were able to determine the degree of crystallinity (Figure 1). These measurements were conducted at 100  $\mu\text{m}$  intervals across the cross-section of the tensile specimens, as shown in the Figure 2. The spatial resolution, in the case of Raman microscopy, is determined by various factors, including the instrument setup, laser wavelength, and optics quality. Typically, Raman microscopy achieves spatial resolutions ranging from a few hundred nanometers to a few

micrometers. Based on the chosen parameters in this study, the Raman resolution in the XY plane was 871 nm, and in the Z-axis, it was 2595 nm. These resolutions of Raman measurements are widely suitable for the chosen step of 100  $\mu\text{m}$ .

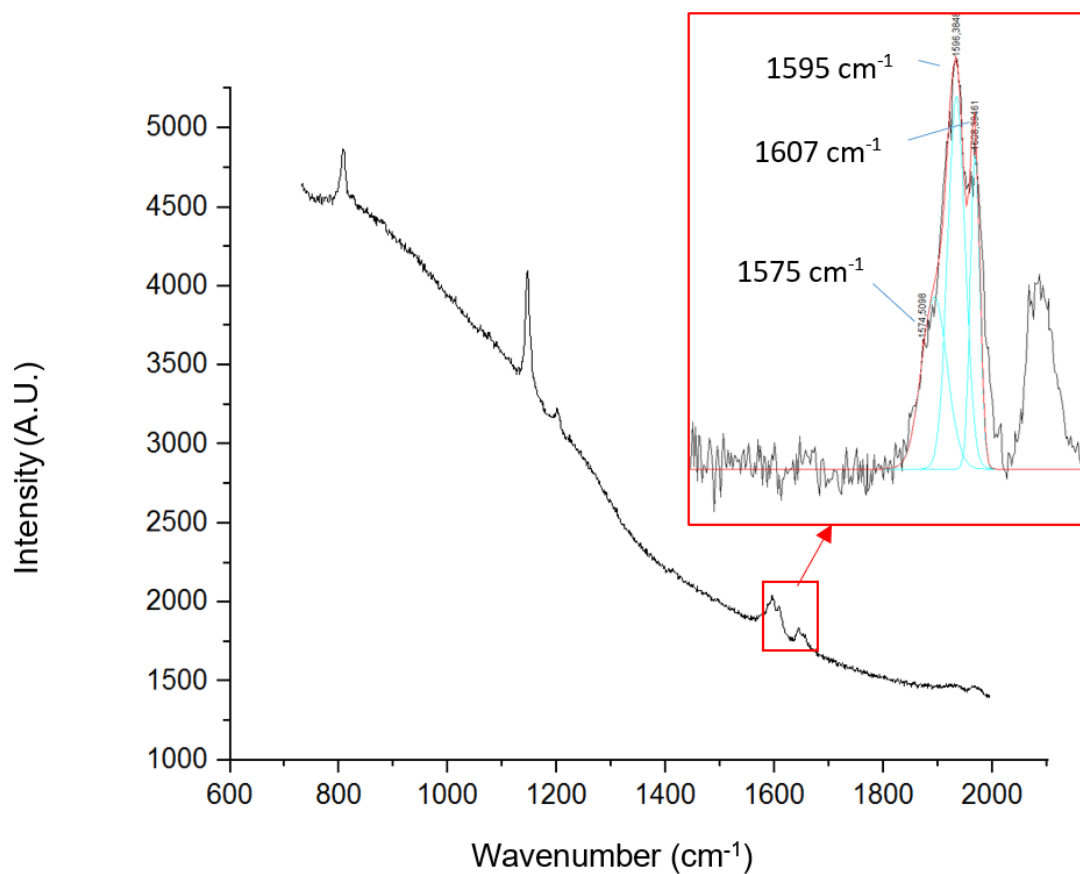


*Figure 1: Raman spectrum of the injected PEEK sample, with the region of interest highlighted in the red box, along with its deconvolution.*

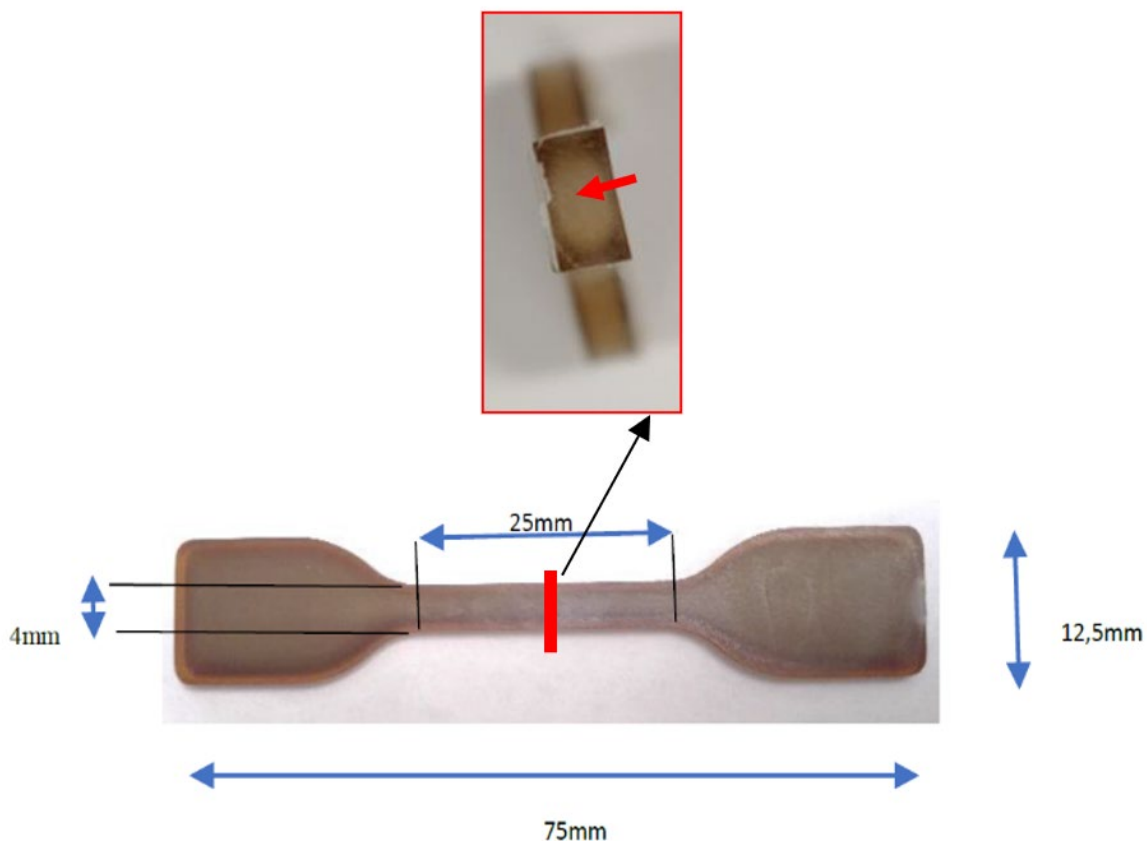


Figure 2: Dimensions of the injected PEEK tensile specimen and its cross-section where the local crystallinity measurements were conducted. The arrow indicates the direction of measurement.

### 2.3. Mechanical properties measuring

The tensile tests were conducted using an INSTRON 3369 tensile machine, following the ISO 527-2 Type 5A standard for specimen preparation. The tensile test speed was taken as 10 mm/min. The aim was to measure the macroscopic tensile properties, which included the elastic modulus, yield strength, stress, and elongation at failure.

Furthermore, nanoindentation tests were conducted on the cross-section of PEEK samples to measure nanoscale mechanical properties at various depths. Indentation cycles of load-hold-unload were performed using a Hysitron Ti950 nanoindenter from Bruker, equipped with a diamond three-sided Berkovich pyramidal tip. A constant strain rate loading (CSR) at  $1 \text{ s}^{-1}$  was applied up to a maximum load of  $400 \mu\text{N}$  (corresponding to approximately 250 nm penetration depth), followed by a hold time of 20 s before unloading. The equipment recorded

the force and penetration depth into the material, allowing for the calculation of the contact stiffness,  $S$ . This was done by fitting the unloading portion of the indentation curve (force-penetration) and taking its derivative at the maximum penetration depth. Subsequently, hardness  $H$  (GPa) and reduced elastic modulus  $E_r$  (GPa) were determined according to the method of Oliver and Pharr [33]. The hardness ( $H$ ) characterizes the material's resistance to plastic deformation under the indentation conditions, while the reduced elastic modulus ( $E_r$ ) represents the combined elastic deformation of both the indented sample and the indenter.

Figure 3 illustrates the nanoindentation samples, indicating the direction of measurement points within the cross-section of each sample. Nanoindentation measurements were conducted on commercial PEEK, injected PEEK, and plasma treated PEEK, with a step size of  $5\ \mu\text{m}$  from the surface to a distance of  $1000\ \mu\text{m}$  within the sample. For the  $180^\circ\text{C}$  annealed PEEK and  $250^\circ\text{C}$  annealed PEEK, nanoindentation measurements were performed with a step size of  $50\ \mu\text{m}$ . Prior to testing, the samples were prepared by polishing the surfaces using silicon carbide grinding papers up to a grit size of 4000, followed by diamond suspensions with particle sizes as small as  $1\ \mu\text{m}$ .

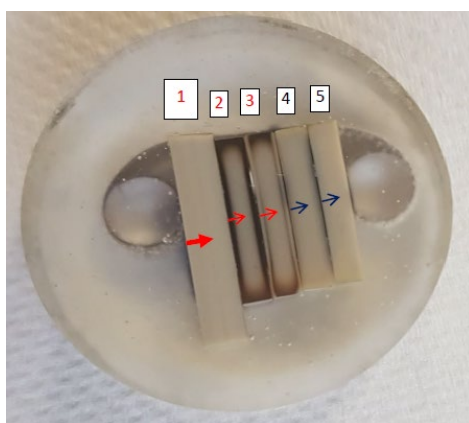


*Figure 3: The PEEK samples prepared for nanoindentation measurements include: 1) commercial PEEK; 2) injected PEEK; 3) plasma-treated injected PEEK; 4)  $180^\circ\text{C}$  annealed PEEK; and 5)  $250^\circ\text{C}$  annealed PEEK. The arrows indicate the direction of the measurements, which were conducted from an edge towards the core of each sample.*

#### **2.4. Scanning Electron Microscopy (SEM)**

The surface topology was observed using a high-resolution Field Emission Scanning Electron Microscope, IT 500 HR from JEOL. Non-conductive samples were coated with a 10 nm thick layer of gold using a JEOL JFC-1200 sputter to facilitate imaging in high vacuum mode ( $10^{-4}$  Pa) with secondary electrons. An acceleration voltage of 20 keV was selected for the imaging process.

A permanganic etching technique was employed to reveal the spherulitic structure and lamellar details on the cross-sectional surface of the PEEK samples [17]. Following the polishing process using silicon carbide papers up to 4000 grit size, the PEEK samples were etched at room temperature by immersing them in a mixture of 1 g of potassium permanganate powder and 40 ml of orthophosphoric acid (approximately 90%) for a duration of 30 minutes. The etching process was terminated by adding hydrogen peroxide, and the samples were subsequently rinsed with distilled water. After completion of the etching procedure, the PEEK samples were air-dried at room temperature for one day prior to SEM observations.

The diameter and the spherulite occupancy rate in the images resulting from SEM observations were estimated using the Perfect Image<sup>®</sup> software. Initially, the image was processed based on grayscale thresholding. In the resulted image, the etched areas were depicted as black, while the spherulite areas appeared as white. Subsequently, the ratio of spherulite areas to the overall image surface was calculated using Perfect Image<sup>®</sup> to obtain the occupancy rate,  $D$ .

### **3. Results and discussion**

#### **3.1. Results of crystallinity measurements**

The results of the crystallinity measurements obtained through density measurements for all PEEK samples are presented in Figure 4. Commercial PEEK and 250°C annealed PEEK samples exhibited the highest global degree of crystallinity, reaching approximately 26%. In

contrast, the injected PEEK samples displayed the lowest crystallinity value, measuring 9.5%. This can be attributed to the high cooling rate employed during the injection molding process, where the intentionally unheated mold resulted in the amorphous state of the surface in the injected PEEK samples, thereby reducing the volume fraction of crystallization. Previous studies utilizing DSC analysis [24,34,35] have demonstrated that the non-isothermal crystallization of PEEK involves a combination of primary fast and secondary slow crystallization processes. The resulting morphology of PEEK depends on the time available for crystallization, which in turn is influenced by the cooling rate. At high cooling rates, only primary crystallization takes place, while secondary crystallization becomes negligible.

The plasma treatment applied to the injected PEEK samples resulted in an increase in the global degree of crystallinity from 9.5% to 14.9%, approaching the value of 16.9% observed in the 180°C annealed samples. This can be attributed to the elevated surface temperature achieved during the plasma treatment. In fact, the surface temperature was measured to locally reach up to 280°C. By raising the temperature above the glass transition temperature of the polymer ( $T_g=143^\circ\text{C}$ ), the macromolecular chains were able to reorganize and promote crystallization.

The 250°C annealed samples exhibited a higher global degree of crystallinity compared to the 180°C annealed samples. This observation aligns with previous studies in the literature, which have shown that increasing the annealing temperature leads to an overall increase in the crystallinity of PEEK specimens. This can be attributed to the enhanced molecular mobility at higher annealing temperatures, which enables the PEEK chains in the amorphous phase to reorient and facilitate the formation of more crystals [36].

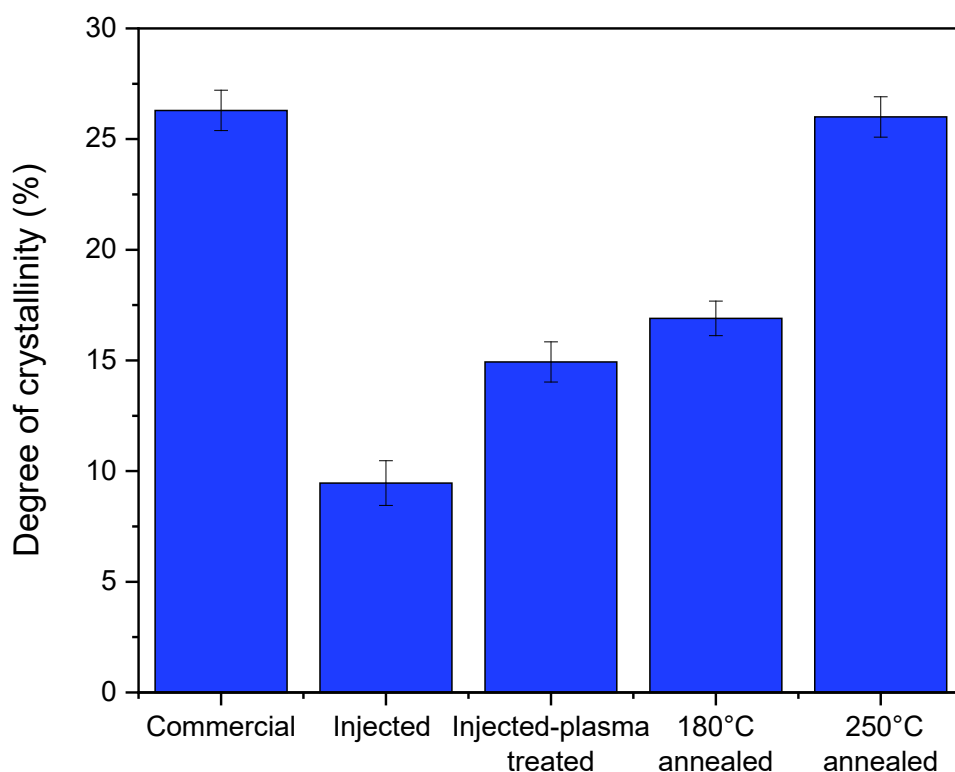


Figure 4: Global degree of crystallinity calculated from the density of the PEEK samples.

According to Seo et al. (2019) [37], the two PEEK grades (600G and 450G) have different molecular weights. The commercial PEEK (600G) has a higher weight-average molecular weight compared to the other PEEK samples injected in our laboratory. As the molecular weight increases, the glass transition temperature ( $T_g$ ) also tends to increase due to the reduced free volume created by chain ends. Therefore, it is expected that the  $T_g$  for 600G is slightly higher than that for 450G. However, the datasheet from the supplier indicates similar  $T_g$  values for both PEEK grades. The figure 4 shows that injected PEEK, when adequately annealed at 250°C, exhibits a similar level of crystallization ratio as the commercial PEEK. Thus, it is used as a reference in this study.

The difference in crystallization is evident through the observed color variation between the PEEK samples, as depicted in Figure 5 for the injected and commercial PEEK. In the cross-

section area of the injected PEEK, a dark brown and slightly translucent layer with a thickness of approximately 400  $\mu\text{m}$  was observed, while the commercial PEEK samples appeared uniformly beige. This color variation serves as an indicator of the crystallinity differences within the cross-section of the PEEK samples. To further investigate this crystallinity variation, Figure 5 presents the local degree of crystallinity obtained through Raman measurements at three specific points in the cross-section: near the surface, approximately 300  $\mu\text{m}$  away from the surface, and at the core point (approximately 1000  $\mu\text{m}$  from surface).

The local crystallinity measurements exhibited a similar trend to the global crystallinity results. Both the commercial and 250°C annealed PEEK samples demonstrated higher local degrees of crystallinity. Additionally, the PEEK samples annealed at 250°C exhibited a higher local degree of crystallinity compared to those annealed at 180°C. The results clearly indicated a significant variation in local crystallinity within the cross-section of the injected PEEK samples, which aligns with the visual observation of color changes.

The plasma treatment of the injected PEEK samples resulted in an increased crystallinity at the surface, except at the selected intermediate point at 300  $\mu\text{m}$ . A distinct impact of the plasma treatment on crystallization is evident when comparing the surface local crystallinity of the injected PEEK samples with that of the plasma-treated injected PEEK samples. The plasma treatment enabled the PEEK surface to regain the degree of crystallinity observed in its core.

Figure 6 illustrates the variation in local crystallinity for the injected and injected plasma-treated PEEK samples, encompassing all the data points. The results corroborate the presence of an amorphous layer on the surface of the injected PEEK samples, extending to a measured depth of 200  $\mu\text{m}$ . Beyond this surface layer, an intermediate region spanning from 200  $\mu\text{m}$  to 400  $\mu\text{m}$  exhibits a progressive increase in the degree of crystallinity until reaching a threshold of approximately 25% in the core.

This variation in crystallinity from the surface to the core is corresponding to the difference in cooling rate in the depth of the sample. During the molding process, molded samples were cooled to room temperature from the melted state, hence, different layers of the sample underwent different cooling rates during solidification. The near-surface layer, in direct contact with the mold, experienced rapid cooling, whereas the core layer had a slower cooling rate. Consequently, the macromolecular chains within the core layer had more time to organize and crystallize, resulting in the observed variation in crystallinity.

The injected plasma-treated PEEK samples exhibited a crystallinity level of approximately 25% within the first 200  $\mu\text{m}$  of depth. However, the impact of the plasma treatment did not extend to the point located at 300  $\mu\text{m}$ , as the degree of crystallinity remained at the same level as the injected PEEK samples. Due to the relatively short duration of the plasma process and the movement of the plasma torch on the surface at a programmed speed, the heat generated by the plasma torch did not have sufficient time to diffuse more deeply into the cross-section of the PEEK sample. In the cross-sectional view of the injected plasma-treated sample (Figure 6), it is evident that an intermediate brown area remains, indicating that this region may not have been significantly affected by the plasma treatment.

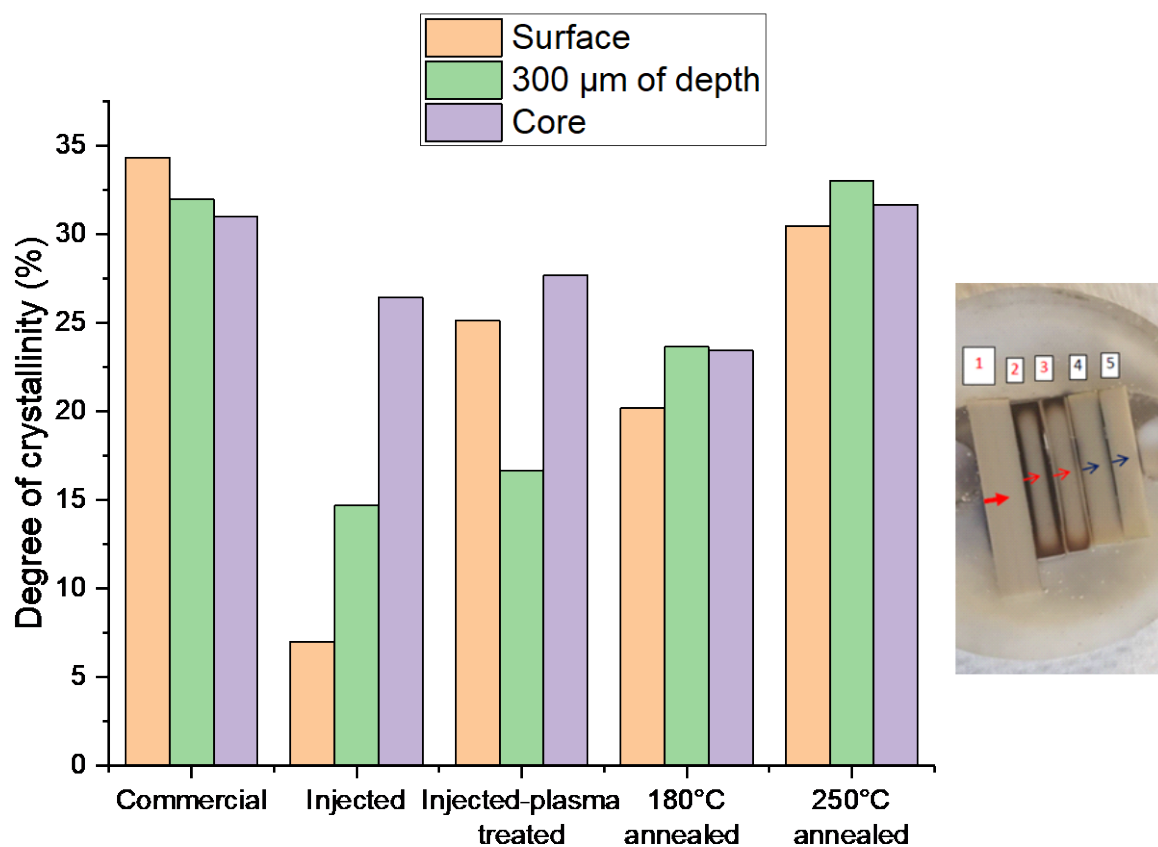


Figure 5: Local degree of crystallinity determined according to Raman's indicator  $A_{1607/1595}$  for the different PEEK samples at the surface, at a 300 μm distance from the surface and in the core of the samples.

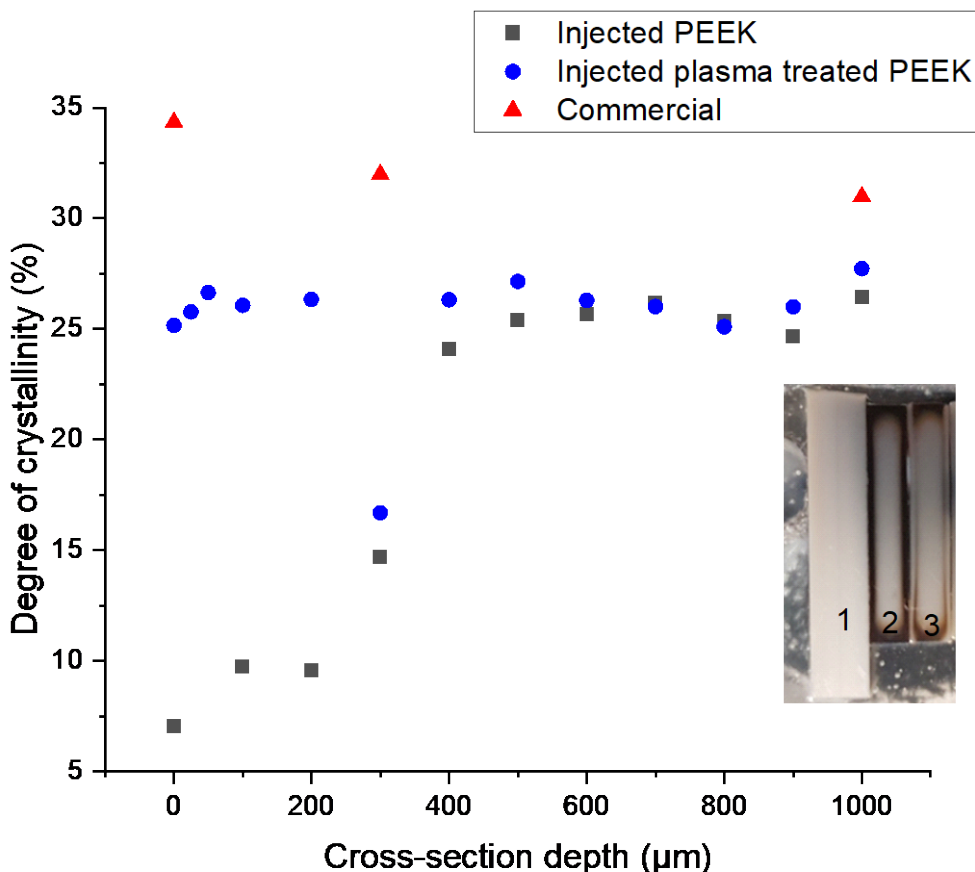


Figure 6: Local degree of crystallinity determined according to Raman's indicator  $A_{1607/1595}$  in the cross-section of the injected PEEK and of the injected plasma treated PEEK. The red slots are reported as a reference for the commercial PEEK sample.

Based on our observations, it can be inferred that the plasma treatment, as conducted with our specific parameters, induced a thermal effect on the surface layer up to a depth of 200  $\mu\text{m}$ , resulting in the structural reorganization of the polymer. It is possible that the temperature within this region exceeded the glass transition temperature of PEEK ( $T_g=143^\circ\text{C}$ ). Many works have reported that cold crystallization in PEEK occurs after exceeding the glass transition temperature [21,38,39]. Depending on the PEEK temperature above the  $T_g$  the cold crystallization is different. According to Ivanov et al. (1999) [40], during the initial stage of cold crystallization (within a low-temperature range below  $T_g+50^\circ\text{C}$ ), only minor lamellar-scale reorganization takes place, resulting in a slight increase in crystal thickness and formation. This limited reorganization is attributed to the slow dynamics of amorphous segments, which hinders significant large-scale rearrangements. However, at higher temperatures, a more

extensive melting/recrystallization mechanism occurs. This process involves the recrystallization of entire lamellar stacks, leading to a state with lower overall free energy and the formation of thicker and denser crystals.

Despite the consistent trend in crystallinity observed using density measurements, it should be noted that the Raman-based degrees of crystallinity obtained in this study had much higher values than those measured by density. For instance, the global degree of crystallinity measured by density for the injected PEEK sample was 9.5%, whereas Raman analysis indicated a range of approximately 7% at the surface to around 25% in the core. In this particular case, the disparity can be partially attributed to the fact that density-based crystallinity considers an average value encompassing the crystallinity of amorphous regions near the surface, transition intermediate region, and semi-crystalline core. However, this explanation cannot be applied to the commercial PEEK and the 250°C annealed PEEK, which respectively, had higher values comparing to those measured by density. This difference may be related to the used correlation curve which is obtained from density measurements and ratios found in the reported work [21]. Further investigation is needed to better understand and reconcile these variations.

### **3.2. Nanoindentation Results**

All of the PEEK samples were characterized using the nanoindentation equipment. Figure 7 and Figure 8 illustrate the hardness ( $H$ ) and reduced elastic modulus ( $E_r$ ) as a function of distance ( $x$ ) across the cross-section, ranging from the surface ( $x=0$ ) to the core ( $x = 1000 \mu\text{m}$ ). The spatial resolution of nanoindentation relies on both the lateral dimensions of the indenter tip and the vertical resolution of the displacement measurement system. This enables localized characterization of mechanical properties at length scales ranging from micro- to nanometers. Considering the measured contact area, the Berkovich Tip resulted in a footprint of approximately 1.5 to 2 micrometers on each of the three sides, which aligns with the chosen indenter step of  $5 \mu\text{m}$ .

Firstly, the nanomechanical results (Er and H) for the commercial PEEK demonstrated a relatively uniform level across the cross-section, represented by a dashed line serving as a reference for the other samples. In the case of injected PEEK, a decrease in both mechanical properties was observed near the surface. Within a distance of approximately  $x \approx 200 \mu\text{m}$ , the elastic modulus and hardness were at their lowest values, gradually increasing through a transition zone until reaching a plateau corresponding to the core value at a distance of  $400 \mu\text{m}$ . The plasma treatment enhanced both the elastic modulus and hardness of the injected PEEK at the surface within a thickness of approximately  $200 \mu\text{m}$ . As indicated by the Raman degree of crystallinity results, the nanomechanical properties were not affected by the plasma treatment for thicknesses greater than  $300 \mu\text{m}$ . Beyond this point, going deeper into the sample, the nanomechanical properties followed exactly the same trend for both the injected PEEK and the injected plasma treated PEEK, indicating that the plasma treatment no longer had an effect ( $x > 300 \mu\text{m}$ ) on the sample. These evolutions in hardness and reduced elastic modulus mirrored those observed in the degree of local crystallinity curves.

The commercial,  $180^\circ\text{C}$  annealed, and  $250^\circ\text{C}$  annealed PEEK samples exhibited noticeably more uniform nanoindentation results throughout the cross-section. The annealing process effectively eliminated the thermal history of the injected PEEK samples and induced recrystallization at different levels based on the annealing temperature. Consequently, the  $250^\circ\text{C}$  annealed PEEK samples displayed slightly higher local mechanical properties compared to the  $180^\circ\text{C}$  annealed PEEK samples.

When considering only the reduced elastic modulus results of the samples, no significant differences were observed between the injected, injected plasma treated, and  $180^\circ\text{C}$  annealed samples in the core region (for  $x > 500 \mu\text{m}$ ). However, the commercial and  $250^\circ\text{C}$  annealed PEEK samples exhibited the highest values for the reduced elastic modulus, which can be attributed to their higher degree of crystallinity.

These nanoindentation results are consistent with the existing literature, which indicates that a higher global crystalline content in PEEK samples corresponds to higher nanoindentation mechanical properties [26,28]. The nanoindentation results showed that injected and plasma injected PEEK samples are essentially inhomogeneous in the cross-section and the results of local mechanical properties do not represent the overall material's behavior. Therefore, it is necessary to examine nanoindentation measurements across the cross-section to assess the variations in mechanical properties. The plasma treatment elevated the mechanical properties at the surface to levels comparable to those in the core, but a residual amorphous layer remained at a depth of approximately 300  $\mu\text{m}$ . This amorphous layer, with lower mechanical properties, may introduce a vulnerability in the assembly of mechanical components and result in premature failure.

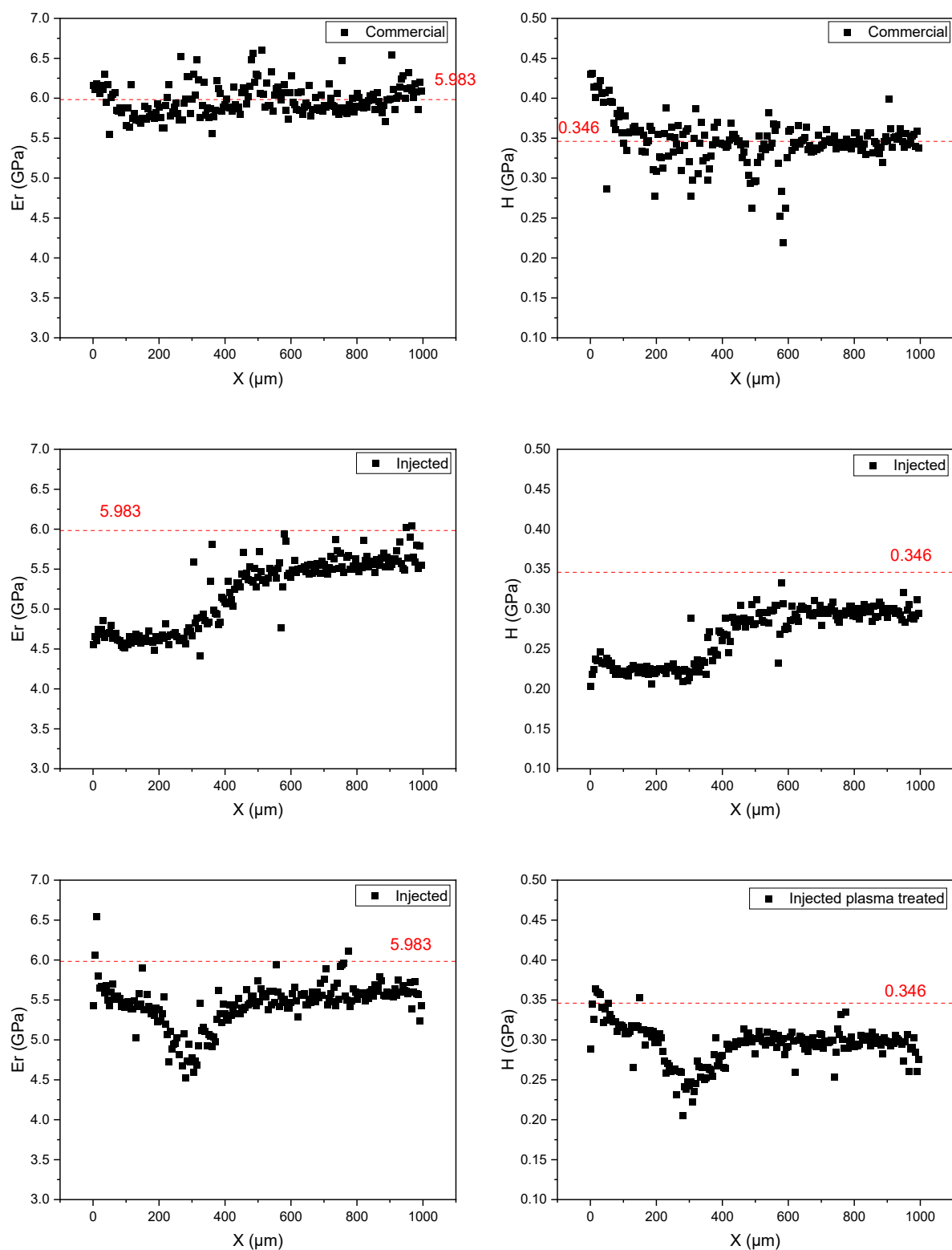


Figure 7: Nanoindentation results: reduced elastic modulus (left) and Hardness (right) for the different PEEK samples. The red dashed line represents the mean values for commercial PEEK and serves as a reference line.

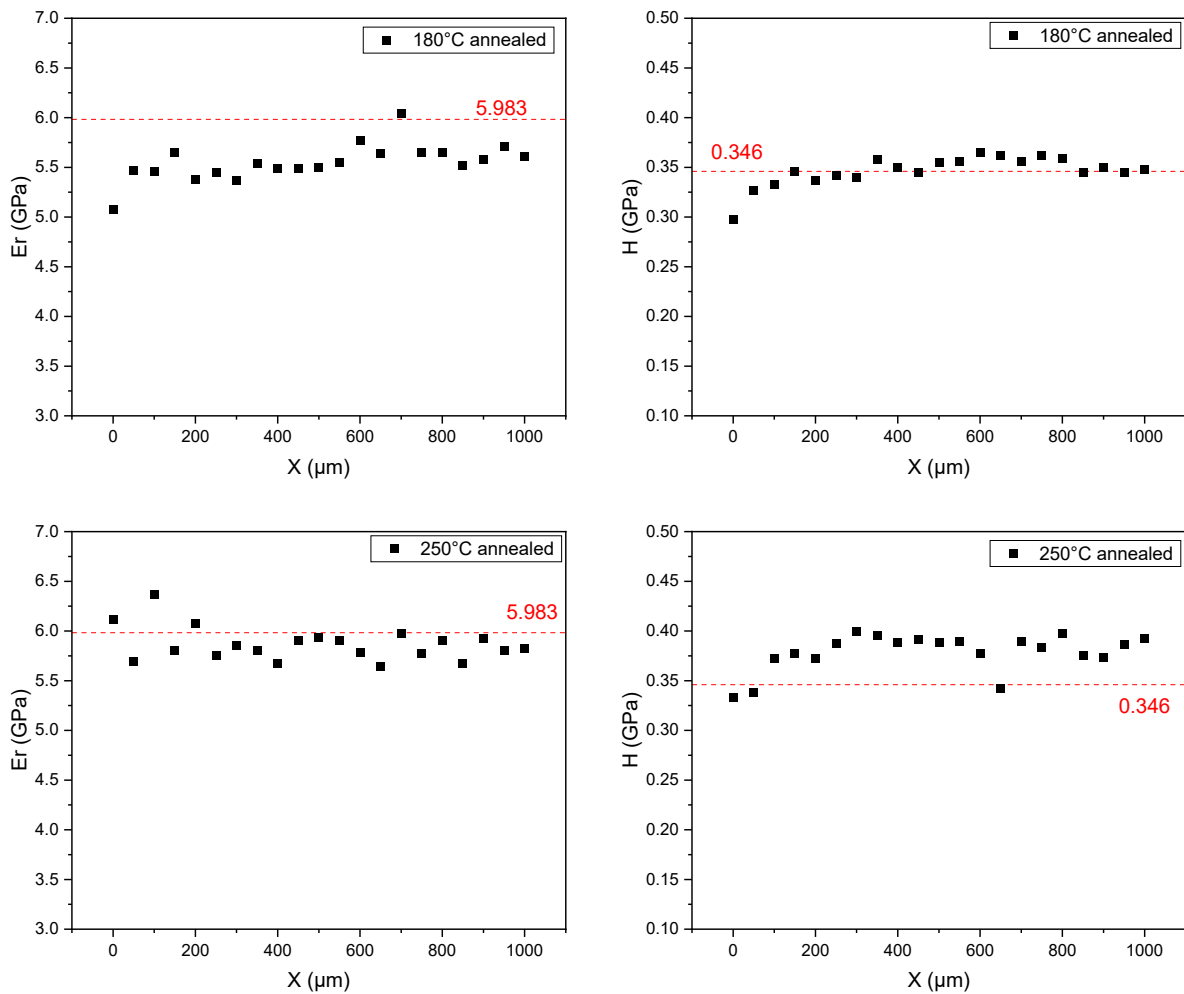


Figure 8: Nanoindentation results: reduced elastic modulus (left) and Hardness (right) for the different PEEK samples. The red dashed line represents the mean values for commercial PEEK and serves as a reference line.

### 3.3. SEM Results: Spherulitic structure

After permanganic etching and metallization of the PEEK samples, the resulting SEM images are presented in Figure 9. Each PEEK sample was examined for its microstructure in the three previously discussed regions in terms of crystallinity ratio and nanomechanical results. Figure 9 displays SEM views at the surface, approximately 300  $\mu\text{m}$  from the surface, and in the core of the samples.

Most of the SEM images exhibit spherulites with varying sizes and densities, except for the surface of the injected PEEK sample where no crystallization is observed. Figure 10 shows

an example to estimate spherulite diameter and occupancy rate, denoted as  $D$ , using Perfect Image<sup>®</sup> Software. All images depict the characteristic morphology of spherulites, forming a Maltese cross pattern (see image (i)).

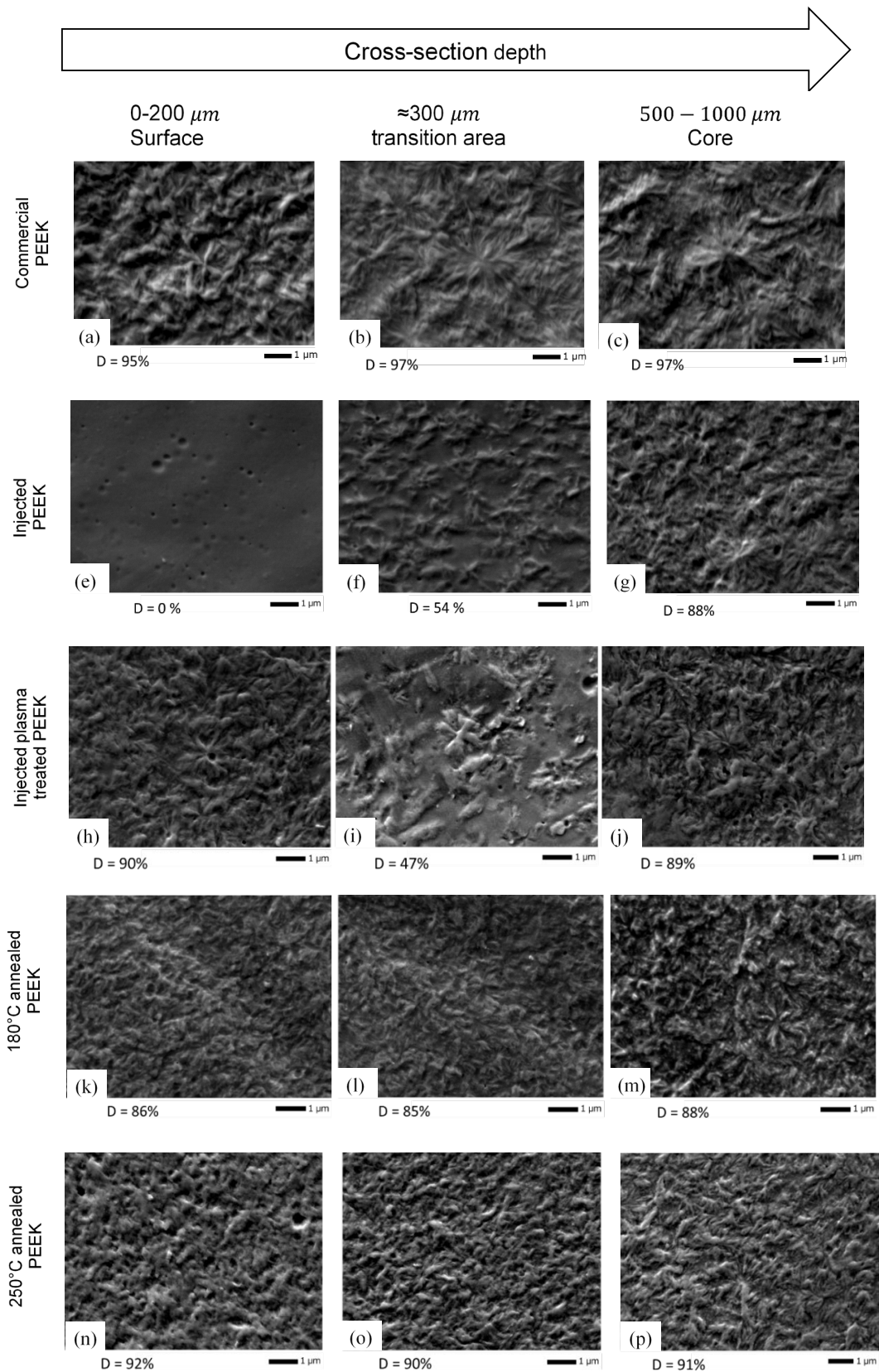


Figure 9: SEM images of the spherulites observed for the different PEEK specimens versus the cross-section. Left: in the surface area vicinity. Middle: at about 300  $\mu\text{m}$  from the surface and Right: in the core of the samples (Secondary electrons, 20kV,  $\times 14000$ ). D: spherulites occupancy rate (error:  $\approx 5\%$ ).

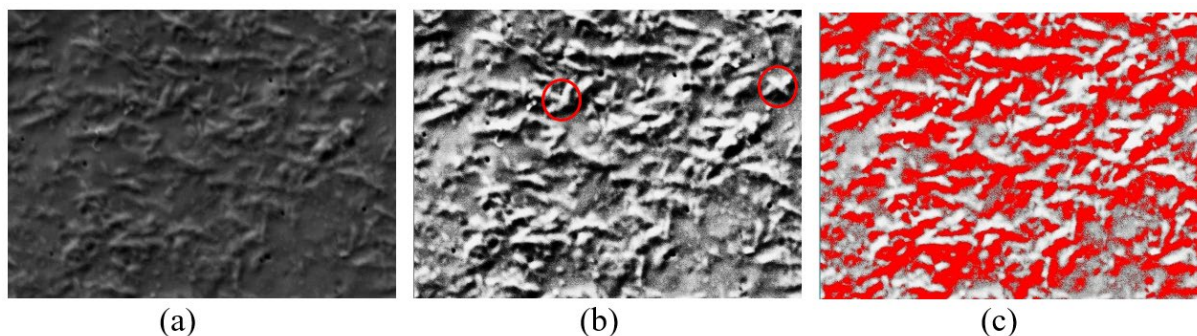


Figure 10: digital estimation of spherulites occupancy rate  $D$  (transition area for injected PEEK;  $D$  was estimated at 54%): (a) original SEM image; (b) contrast modification and diameter measure by Perfect Image<sup>®</sup>; (c) phase estimation after processing by Perfect Image<sup>®</sup>)

Commercial, 180°C annealed and 250°C annealed PEEK samples revealed homogeneous microstructures with a constant spherulitic density consistent the 3 areas examined. However, the images of commercial PEEK appeared to show larger spherulites (approximately 2.75  $\mu\text{m}$  in diameter) that were less numerous, resulting in a higher occupancy rate. On the other hand, the 180°C annealed and 250°C annealed PEEK samples displayed smaller spherulites (around 1  $\mu\text{m}$  in diameter) with a favorable occupancy rate. This difference in microstructure may be attributed to variations in the thermal kinetics during the manufacturing processes. The commercial PEEK, produced through a plate production process involving hot crystallization from a melted state, exhibited distinct characteristics compared to the annealed samples. The annealed PEEK samples, subjected to a bulk annealing process involving cold crystallization from a glass state as described in the methodology section, displayed a different pattern of spherulite formation.

In contrast, SEM images for injected samples and plasma treated samples showed a significant variation in crystallinity throughout the cross-section. A clear difference of spherulites presence was observed among the surface, transition area, and core regions of injected PEEK. Specifically, no spherulites were detected at the surface, while the core displayed a spherulite structure comparable to that of annealed samples. The plasma treatment

let the spherulites growing up from the amorphous surface. It is worth noting that even with this observation of spherulites, the area at 300  $\mu\text{m}$  exhibited a lower crystallization density ( $D = 54\%$  - image f and  $D = 47\%$  - image i) for injected PEEK and injected plasma-treated PEEK, respectively. This characterization of spherulites aligns with the local degree of crystallization (Figure 6) and the nanomechanical results (Figure 7). The observed growth of spherulites with SEM corresponded to higher local crystallization rates measured by Raman spectroscopy and higher nanomechanical properties determined by nanoindentation. This correlation held true for the three areas: near the surface (0 to 200  $\mu\text{m}$ ), the intermediate area (300  $\mu\text{m}$ ), and the core (beyond 400  $\mu\text{m}$ ). The impact of the plasma treatment on the amorphous injected PEEK was thus evident through the recovery of spherulite density near the surface.

To provide an overview, we have compiled all the results of local crystallinity measured by Raman spectroscopy, elastic modulus obtained from nanoindentation, and SEM observations of spherulites in the cross-section in Figure 11. The figure demonstrates a consistent trend among the results obtained from the three techniques for injected PEEK and injected plasma-treated PEEK. These findings are in line with previous studies that have established a connection between the local mechanical properties of the PEEK surface and its crystallinity ratio. A higher crystallinity ratio was found to correspond to increased values of reduced elastic modulus and hardness [26–30]. This study not only established the correlation between local mechanical variations and local crystallinity at the surface of PEEK, but also extended it to the cross-section of the material. The observed variations can be attributed to the uneven cooling rates experienced within the cross-section during the solidification process. Rapid cooling at the surface resulted in lower crystallinity and subsequently lower mechanical properties, whereas slower cooling in the core led to higher crystallinity and enhanced mechanical properties. This trend was also evident in the hardness measurements obtained through nanoindentation. In the case of plasma surface treatment, the temperature diffusion

caused the polymer to recrystallize within a thickness of 200  $\mu\text{m}$  in our study, thereby altering the local mechanical responses. These changes may induce mechanical stresses.

The correlation between the local degree of crystallinity determined by Raman spectroscopy and the reduced elastic modulus measured via nanoindentation is depicted in Figure 12. The quadratic fitting of the data demonstrated a strong nonlinear correlation with  $R^2$  value of 0.889. Linear correlation has been observed in previous studies [24] where an increase in annealing temperature resulted in higher crystallinity content (varying from 30% to 40% for other grade of PEEK) and subsequently an increase in the reduced elastic modulus. However, these studies do not take lower content of crystallinity (<30%). The nonlinear nature of this correlation, as indicated by the Figure 12, would need further investigation with additional results obtained from the cross-section of the sample. However, the correlation between the crystallinity and the nanoindentation results for PEEK is demonstrated.

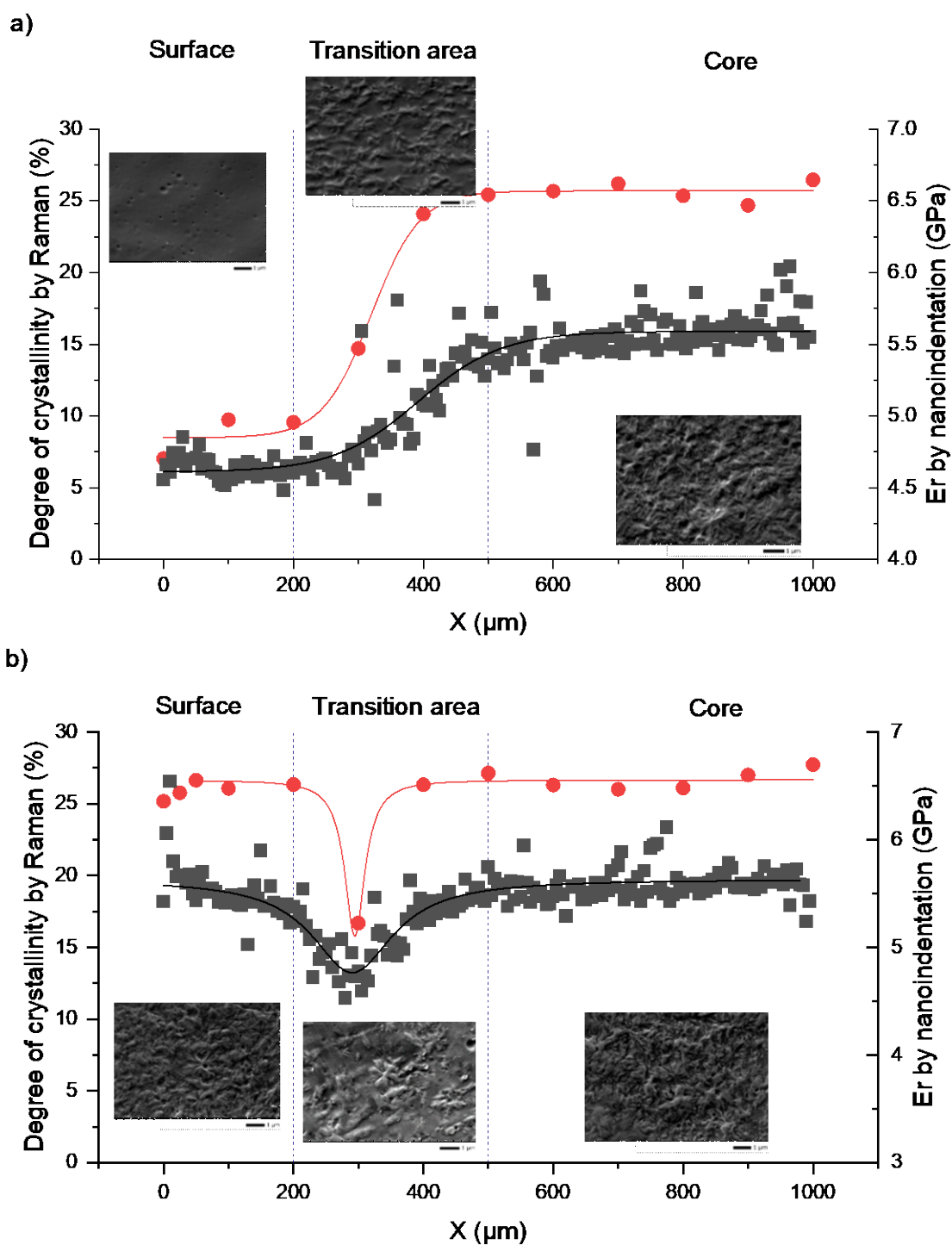


Figure 11: Correlation between the reduced elastic modulus and the Raman degree of crystallinity for the injected samples (a) and injected plasma treated samples (b). The corresponding SEM images as described on Figure 9 are respectively reported on the different areas of the cross-sections. Dashed lines are guides for eyes.

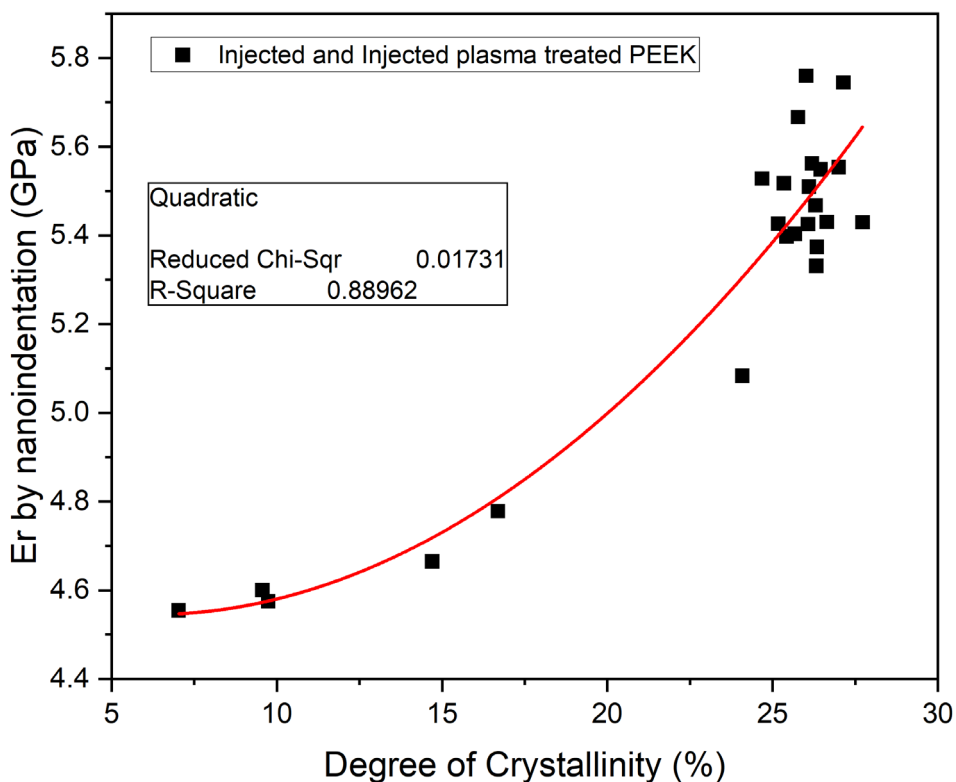


Figure 12: correlation between the reduced elastic modulus measured via nanoindentation and the local degree of crystallinity determined by Raman spectroscopy.

### 3.4. Effects of the crystallization on the global mechanical results

The macroscopic mechanical characteristics of the various PEEK samples were investigated by analyzing their tensile stress-strain curves, as illustrated in Figure 13 and summarized in Table 1.

As highlighted by many works [23,24], by comparing 250°C annealed samples to 180°C annealed ones, the higher annealing temperature improved gradually the elastic modulus, yield strength and failure stress, attaining the values of commercial PEEK. However, increasing the annealing temperature also led to a rapid decrease in the failure elongation. This behavior can be attributed to the corresponding increase in the global degree of crystallinity, which rose from 16.9% for the 180°C annealed samples to 26% for the samples annealed at 250°C.

As expected, the injected PEEK samples, which exhibited the lowest global degree of crystallinity (9.46%), demonstrated the lowest values of elastic modulus, yield strength, and failure stress, while exhibiting the highest failure elongation. This can be attributed to the presence of an amorphous layer (200  $\mu\text{m}$ ) on the surface of the injected PEEK samples, which contributed to the degradation of the overall mechanical properties compared to the other PEEK samples. The plasma treatment of the injected PEEK resulted in an increase in the tensile properties, including the elastic modulus, yield strength, and failure stress. This improvement can be attributed to the recrystallization of the surface, which led to an increase in the global degree of crystallinity to 15%. However, despite these enhancements, the presence of the remaining amorphous layer in the cross-section, as previously observed at 300  $\mu\text{m}$ , limited the overall changes in the mechanical properties compared to other PEEK samples. These findings highlight the significance of even a thin amorphous layer within the PEEK thickness, as it can significantly affect the global mechanical behavior of the polymer.

Various studies have indicated that the elastic modulus values obtained through nanoindentation for polymers are generally higher compared to those measured through tensile tests [41,42]. This phenomenon was clearly observed in this study in the case of annealed PEEK samples at 180°C (mean value of nanoindentation  $E_r = 5.67 \text{ GPa} > \text{traction value } E = 3.8 \text{ GPa}$ ) and 250°C (5.82 GPa > 3.96 GPa), where the crystallinity is homogeneous across the cross-section. This difference was attributed to the limitations of the Olivier and Pharr procedure for

polymer indentation, which is influenced by their unique viscoelastic mechanical behavior [41,42].

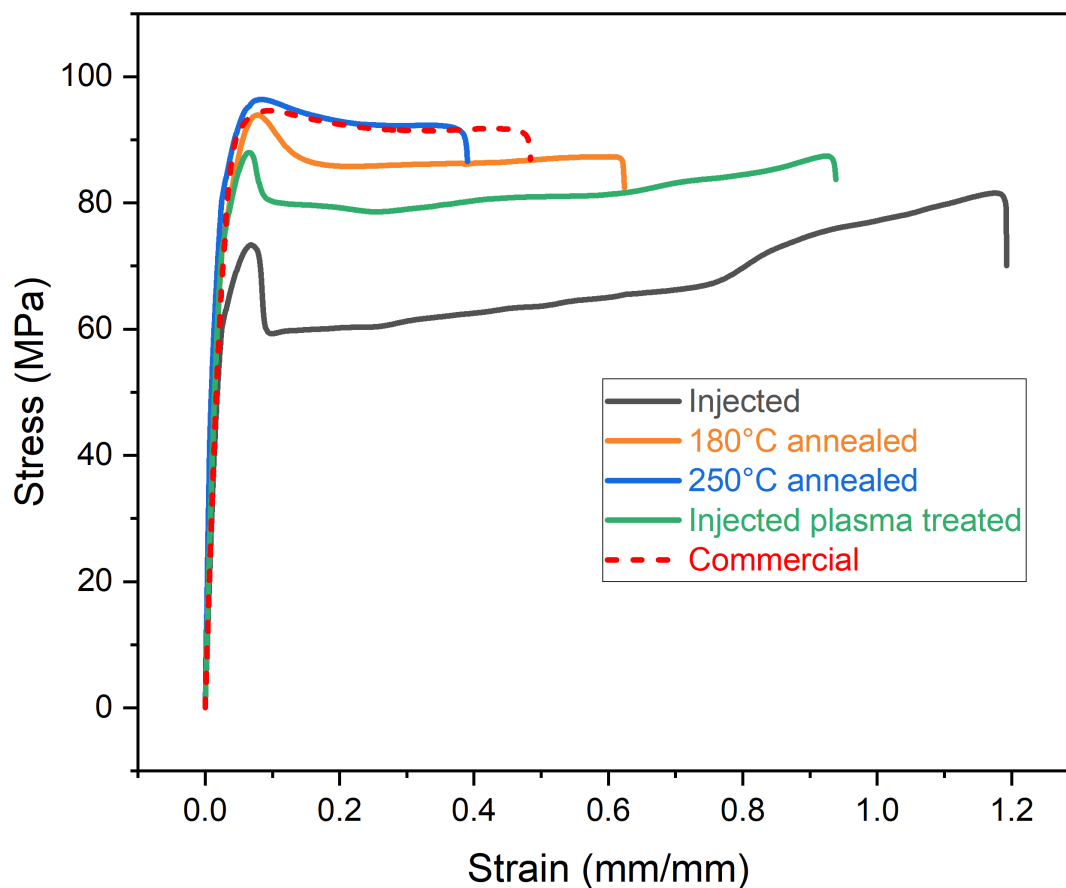


Figure 13: Stress-strain curves

Table 1: Stress-strain tests results

| PEEK samples                 | E- Modulus of elasticity [GPa] | Yield strength [MPa] | Failure stress [MPa] | Failure elongation [%] |
|------------------------------|--------------------------------|----------------------|----------------------|------------------------|
| Commercial                   | 3.7 ( $\pm 0.5$ )              | 95 ( $\pm 1.1$ )     | 89 ( $\pm 1.3$ )     | 45 ( $\pm 7$ )         |
| 250°C annealed PEEK          | 3.96 ( $\pm 0.6$ )             | 95.3 ( $\pm 1.2$ )   | 90.7 ( $\pm 1.5$ )   | 39.1 ( $\pm 6.1$ )     |
| 180°C annealed PEEK          | 3.8 ( $\pm 0.2$ )              | 93.8 ( $\pm 1.1$ )   | 86.9 ( $\pm 1.2$ )   | 51.2 ( $\pm 11$ )      |
| Injected plasma treated PEEK | 3.64 ( $\pm 0.4$ )             | 88.8 ( $\pm 1.5$ )   | 88.2 ( $\pm 2$ )     | 90.7 ( $\pm 14$ )      |
| Injected PEEK                | 3.16 ( $\pm 0.1$ )             | 71 ( $\pm 2.9$ )     | 80.9 ( $\pm 3.3$ )   | 117.4 ( $\pm 5.4$ )    |

#### 4. Conclusion

In this study, we investigated the impact of plasma treatment on the crystallization ratio of PEEK. By creating a gradient of crystallization within the PEEK samples using an injection molding process, we were able to compare the global and local degree of crystallinity among different samples, including commercial PEEK, injected PEEK, plasma-treated PEEK, and annealed PEEK. Our results showed that the global degree of crystallinity decreased from approximately 26% for commercial PEEK to 9.5% for injected samples. This decrease was attributed to the surface amorphization of injected PEEK, which extended to a thickness of around 400  $\mu\text{m}$  from the surface of the samples. Raman spectrometry provided further insight into the variation of crystallinity from the surface to the core of injected PEEK.

An optimized plasma treatment, typically employed to enhance polymer adhesion, was applied to the injected PEEK samples. This treatment resulted in a significant increase in the crystallization ratio of the injected PEEK, restoring it to approximately 25% within a depth of approximately 200  $\mu\text{m}$ , which corresponds to the crystallinity ratio in the core of the samples. However, a thin layer of material located around 300  $\mu\text{m}$  remained unaffected by the plasma treatment, maintaining a degree of crystallinity of approximately 15%. In order to validate this temperature effect, we showed that annealing the injected PEEK samples to temperatures of 180 °C and 250°C increased the global crystallization ratio respectively to a mean of 16.9% and 26%. Interestingly, no further variations in the crystallization ratio were observed across the cross-section of the samples after annealing.

We established a correlation between the changes in crystallization ratio and the nanoindentation measurements. The reduced elastic modulus and hardness exhibited a similar trend to the local crystallinity ratio measured by Raman spectroscopy. Specifically, the local mechanical properties of the injected PEEK experienced a significant decrease at the surface,

consistent with the local crystallization ratio. In contrast, the injected plasma-treated PEEK demonstrated an improvement in mechanical properties within a depth of approximately 200  $\mu\text{m}$  from the surface, aligning with the crystallization modifications induced by the plasma treatment. Furthermore, the annealing process effectively eliminated the thermal history of the injected PEEK and led to different levels of recrystallization depending on the annealing temperature.

Our study successfully established a correlation between the density of spherulites observed using SEM at a micrometer scale, the local crystallization ratio measured by Raman spectroscopy, and its variation across the sample cross-section. This crystallization ratio was further linked to changes in local mechanical properties determined by nanoindentation. Especially, we demonstrated that the overall mechanical behavior of the different samples was directly influenced by these local crystallinity and mechanical properties.

The findings emphasized the relevance of the employed techniques in investigating variations in crystallinity and their correlation with the local mechanical behavior of the polymer. Understanding such variations is crucial in assessing the strength of mechanical assemblies. Even a small or tiny layer with altered crystallinity on the surface (injected PEEK) or in the cross-section (injected plasma-treated PEEK) can weaken the mechanical integrity of assembled parts, leading to cohesive failure. Crystallization changes can occur once the local temperature reaches the glass transition temperature of the polymer. This aspect is particularly critical for non-technical polymers like PE, PP, PA, as they have significantly lower glass transition temperatures compared to PEEK. Additionally, the studied modification of crystallinity may occur even in already crystallized polymers, where the spherulitic density is not at its maximum.

## **5. Acknowledgments**

The authors would like to thank the NanoMeca platform from ScanMAT, UAR 2025 Univ Rennes-CNRS for the nanoindentation investigation. Part of this work was financially supported by the European Union (ERDF), the French Ministry for Higher education, the Brittany region and Rennes Métropole through the CPER Projects PRIN2TAN and GLASS.

## 6. References

- [1] R. Stewart, Thermoplastic composites - Recyclable and fast to process, *Reinf. Plast.* 55 (2011) 22–28. [https://doi.org/10.1016/S0034-3617\(11\)70073-X](https://doi.org/10.1016/S0034-3617(11)70073-X).
- [2] M. Nagalakshmaiah, S. Afrin, R.P. Malladi, S. Elkoun, M. Robert, M.A. Ansari, A. Svedberg, Z. Karim, Biocomposites: Present trends and challenges for the future, *Green Compos. Automot. Appl.* (2018) 197–215. <https://doi.org/10.1016/B978-0-08-102177-4.00009-4>.
- [3] V. Mittal, *High Performance Polymers and Engineering Plastics*, 2011. <https://doi.org/10.1002/9781118171950>.
- [4] C.K. aa. Akkan, M.E. i. Hammadeh, A. May, H.W. Park, H. Abdul-Khaliq, T. Strunskus, O.C. en. Aktas, Surface topography and wetting modifications of PEEK for implant applications, *Lasers Med. Sci.* 29 (2014) 1633–1639. <https://doi.org/10.1007/s10103-014-1567-7>.
- [5] M. Escobar, B. Henriques, M.C. Fredel, F.S. Silva, M. Özcan, J.C.M. Souza, Adhesion of PEEK to resin-matrix composites used in dentistry: a short review on surface modification and bond strength, *J. Adhes. Sci. Technol.* 34 (2020) 1241–1252. <https://doi.org/10.1080/01694243.2019.1706797>.
- [6] L. Hallmann, A. Mehl, N. Sereno, C.H.F. Hämmerle, The improvement of adhesive

- properties of PEEK through different pre-treatments, *Appl. Surf. Sci.* 258 (2012) 7213–7218. <https://doi.org/10.1016/j.apsusc.2012.04.040>.
- [7] B. Wang, M. Huang, P. Dang, J. Xie, X. Zhang, X. Yan, PEEK in Fixed Dental Prostheses: Application and Adhesion Improvement, *Polymers (Basel)*. 14 (2022) 1–19. <https://doi.org/10.3390/polym14122323>.
- [8] S. Singh, C. Prakash, H. Wang, X. feng Yu, S. Ramakrishna, Plasma treatment of polyether-ether-ketone: A means of obtaining desirable biomedical characteristics, *Eur. Polym. J.* 118 (2019) 561–577. <https://doi.org/10.1016/j.eurpolymj.2019.06.030>.
- [9] M. Fedel, V. Micheli, M. Thaler, F. Awaja, Effect of nitrogen plasma treatment on the crystallinity and self-bonding of polyetheretherketone (PEEK) for biomedical applications, *Polym. Adv. Technol.* 31 (2020) 240–247. <https://doi.org/10.1002/pat.4764>.
- [10] M. Behnecke, V. Steinert, S. Petersen, Surface Characterisation of PEEK and Dentin, Treated with Atmospheric Non-Thermal PDD Plasma, Applicable for Dental Chair-Side Procedures, *Plasma*. 4 (2021) 389–398. <https://doi.org/10.3390/plasma4030028>.
- [11] D. Gravis, F. Poncin-Epaillard, J.-F. Coulon, Correlation between the surface chemistry, the surface free energy and the adhesion of metallic coatings onto plasma-treated Poly(ether ether ketone), *Appl. Surf. Sci.* 501 (2020). <https://doi.org/10.1016/j.apsusc.2019.144242>.
- [12] J.-F. Coulon, D. Debarnot, F. Poncin-Epaillard, Plasma texturing of polymers, in: *Eng. Mater.* Springer, 2021: pp. 91–120.
- [13] D. Gravis, G. Rigolé, M. Yengui, W. Knapp, J.F. Coulon, F. Poncin-Epaillard,

- Enhancement of metal adhesion, owing to the plasma texturing of PEEK, *Plasma Process. Polym.* 18 (2021). <https://doi.org/10.1002/ppap.202100009>.
- [14] Z. Zhang, H. Zeng, Effects of thermal treatment on poly(ether ether ketone), *Polymer (Guildf)*. 34 (1993) 3648–3652. [https://doi.org/10.1016/0032-3861\(93\)90049-G](https://doi.org/10.1016/0032-3861(93)90049-G).
- [15] R.S.P. Y. Lee, Effects of Thermal History on Crystallization of Poly(ether ether ketone) (PEEK), *Macromolecules*. 21 (1988) 2770–2776. <https://doi.org/10.1002/app.1968.070120811>.
- [16] D.C. Bassett, R.H. Olley, I.A.M. Al Raheil, On crystallization phenomena in PEEK, *Polymer (Guildf)*. 29 (1988) 1745–1754. [https://doi.org/10.1016/0032-3861\(88\)90386-2](https://doi.org/10.1016/0032-3861(88)90386-2).
- [17] R.H. Olley, D.C. Bassett, D.J. Blundell, Permanganic etching of PEEK, *Polymer (Guildf)*. 27 (1986) 344–348. [https://doi.org/10.1016/0032-3861\(86\)90147-3](https://doi.org/10.1016/0032-3861(86)90147-3).
- [18] S. Kumar, D.P. Anderson, W.W. Adams, Crystallization and morphology of poly(aryl-ether-ether-ketone), *Polymer (Guildf)*. 27 (1986) 329–336. [https://doi.org/10.1016/0032-3861\(86\)90145-X](https://doi.org/10.1016/0032-3861(86)90145-X).
- [19] M. Dosière, C. Fougnes, M.H.J. Koch, J. Roovers, Lamellar morphology of narrow PEEK fractions crystallized from the glassy state and from the melt, *ACS Symp. Ser.* 739 (1999) 166–186. <https://doi.org/10.1021/bk-2000-0739.ch011>.
- [20] A. Jonas, R. Legras, J.P. Issi, Differential scanning calorimetry and infra-red crystallinity determinations of poly(aryl ether ether ketone), *Polymer (Guildf)*. 32 (1991) 3364–3370. [https://doi.org/10.1016/0032-3861\(91\)90540-Y](https://doi.org/10.1016/0032-3861(91)90540-Y).
- [21] M. Doumeng, L. Makhlouf, F. Berthet, O. Marsan, K. Delbé, J. Denape, F. Chabert, A

- comparative study of the crystallinity of polyetheretherketone by using density, DSC, XRD, and Raman spectroscopy techniques, *Polym. Test.* 93 (2021) 106878.  
<https://doi.org/10.1016/j.polymertesting.2020.106878>.
- [22] M. Doumeng, F. Ferry, K. Delbé, T. Mérian, F. Chabert, F. Berthet, O. Marsan, V. Nassiet, J. Denape, Evolution of crystallinity of PEEK and glass-fibre reinforced PEEK under tribological conditions using Raman spectroscopy, *Wear.* 426–427 (2019) 1040–1046. <https://doi.org/10.1016/j.wear.2018.12.078>.
- [23] P. Cebe, S.Y. Chung, S. -D Hong, Effect of thermal history on mechanical properties of polyetheretherketone below the glass transition temperature, *J. Appl. Polym. Sci.* 33 (1987) 487–503. <https://doi.org/10.1002/app.1987.070330217>.
- [24] M. Regis, A. Bellare, T. Pascolini, P. Bracco, Characterization of thermally annealed PEEK and CFR-PEEK composites: Structure-properties relationships, *Polym. Degrad. Stab.* 136 (2017) 121–130. <https://doi.org/10.1016/j.polymdegradstab.2016.12.005>.
- [25] D. Yang, Y. Cao, Z. Zhang, Y. Yin, D. Li, Effects of crystallinity control on mechanical properties of 3D-printed short-carbon-fiber-reinforced polyether ether ketone composites, *Polym. Test.* 97 (2021) 107149.  
<https://doi.org/10.1016/j.polymertesting.2021.107149>.
- [26] T. Iqbal, B.J. Briscoe, S. Yasin, P.F. Luckham, Nanoindentation response of poly(ether ether ketone) surfaces-A semicrystalline bimodal behavior, *J. Appl. Polym. Sci.* 130 (2013) 4401–4409. <https://doi.org/10.1002/app.39723>.
- [27] N.J. R. Powles, D. McKenzie, S. Meure, M. Swain, Nanoindentation response of PEEK modified by mesh-assisted plasma immersion ion implantation, *Surf. Coatings Technol.* 201 (2007) 7961–7969.

- [28] G.Z. Voyiadjis, A. Samadi-Dooki, L. Malekmoitei, Nanoindentation of high performance semicrystalline polymers: A case study on PEEK, *Polym. Test.* 61 (2017) 57–64. <https://doi.org/10.1016/j.polymertesting.2017.05.005>.
- [29] A.M. Díez-pascual, M.A. Gómez-fatou, F. Ania, Nanoindentation in polymer nanocomposites, *Prog. Mater. Sci.* 67 (2015) 1–94. <https://doi.org/10.1016/j.pmatsci.2014.06.002>.
- [30] S.E. Arevalo, L.A. Pruitt, Nanomechanical analysis of medical grade PEEK and carbon fiber-reinforced PEEK composites, *J. Mech. Behav. Biomed. Mater.* 111 (2020) 104008. <https://doi.org/10.1016/j.jmbbm.2020.104008>.
- [31] L. Martineau, F. Chabert, B. Boniface, G. Bernhart, Effect of interfacial crystalline growth on autohesion of PEEK, *Int. J. Adhes. Adhes.* 89 (2019) 82–87. <https://doi.org/10.1016/j.ijadhadh.2018.11.013>.
- [32] D.J. Blundell, B.N. Osborn, The morphology of poly(aryl-ether-ether-ketone), *Polymer (Guildf)*. 24 (1983) 953–958. [https://doi.org/10.1016/0032-3861\(83\)90144-1](https://doi.org/10.1016/0032-3861(83)90144-1).
- [33] W.C. Oliver G.M. Pharr, An improved technique for determining hardness and elastic modulus using load and displacement sensing indentation experiments, *J. Mater. Res.* 7 (1992) 1564.
- [34] M. Regis, M. Zanetti, M. Pressacco, P. Bracco, Opposite role of different carbon fiber reinforcements on the non-isothermal crystallization behavior of poly(etheretherketone), *Mater. Chem. Phys.* 179 (2016) 223–231. <https://doi.org/10.1016/j.matchemphys.2016.05.034>.
- [35] M. Chen, C.T. Chung, Crystallinity of isothermally and nonisothermally crystallized

- poly(ether ether ketone) composites, *Polym. Compos.* 19 (1998) 689–697.  
<https://doi.org/10.1002/pc.10141>.
- [36] Z. Jiang, P. Liu, H.J. Sue, T. Bremner, Effect of annealing on the viscoelastic behavior of poly(ether-ether-ketone), *Polymer (Guildf)*. 160 (2019) 231–237.  
<https://doi.org/10.1016/j.polymer.2018.11.052>.
- [37] J. Seo, A.M. Gohn, O. Dubin, H. Takahashi, H. Hasegawa, R. Sato, A.M. Rhoades, R.P. Schaake, R.H. Colby, Isothermal crystallization of poly(ether ether ketone) with different molecular weights over a wide temperature range, *Polym. Cryst.* 2 (2019).  
<https://doi.org/10.1002/pcr2.10055>.
- [38] C. Bas, A.C. Grillet, F. Thimon, N.D. Alb rola, Crystallization kinetics of poly(aryl ether ether ketone): Time-temperature-transformation and continuous-cooling-transformation diagrams, *Eur. Polym. J.* 31 (1995) 911–921.  
[https://doi.org/10.1016/0014-3057\(95\)00060-7](https://doi.org/10.1016/0014-3057(95)00060-7).
- [39] C. Fougny, M. Dosiere, M.H.J. Koch, J. Roovers, Cold crystallization of narrow molecular weight fractions of PEEK, *Macromolecules*. 32 (1999) 8133–8138.  
<https://doi.org/10.1021/ma9909206>.
- [40] D.A. Ivanov, R. Legras, A.M. Jonas, The crystallization of poly(aryl-ether-ether-ketone) (PEEK): Reorganization processes during gradual reheating of cold-crystallized samples, *Polymer (Guildf)*. 41 (2000) 3719–3727.  
[https://doi.org/10.1016/S0032-3861\(99\)00549-2](https://doi.org/10.1016/S0032-3861(99)00549-2).
- [41] D. Tranchida, S. Piccarolo, J. Loos, A. Alexeev, Mechanical characterization of polymers on a nanometer scale through nanoindentation. A study on pile-up and viscoelasticity, *Macromolecules*. 40 (2007) 1259–1267.

<https://doi.org/10.1021/ma062140k>.

- [42] P.E. Mazeran, M. Beyaoui, M. Bigerelle, M. Guigon, Determination of mechanical properties by nanoindentation in the case of viscous materials, *Int. J. Mater. Res.* 103 (2012) 715–722. <https://doi.org/10.3139/146.110687>.